JOURNAL OF THERMOPHYSICS AND HEAT TRANSFER
Vol. 18, No. 3, July–September 2004

Thermal Joint Resistances of Nonconforming Rough Surfaces with Gas-Filled Gaps

M. Bahrami,* M. M. Yovanovich,† and J. R. Culham‡
University of Waterloo, Waterloo, Ontario, Canada N2L 3G1

An approximate analytical model is developed for predicting the thermal contact resistance of spherical rough solids with the presence of interstitial gases. The joint resistance includes four thermal resistances, that is, macrogap, microgap, macrocontact, and microcontacts. Simple relationships are derived for each component of the joint resistance assuming contacting surfaces are of uniform temperature and that the microgap heat transfer area and the macrocontact area are identical. Effects of main input contact parameters on the joint resistance are studied. It is demonstrated that a surface curvature exists that minimizes the joint resistance for a fixed contact. The model covers all regimes of gas heat conduction modes from continuum to free molecular. The present model is compared with 110 experimental data points and good agreement is shown over entire range of the comparison.

Nomenclature

A	=	area, m^2
a	=	radius of contact, m
b_L	=	specimens radius, m
c_1	=	Vickers microhardness coefficient, Pa
c_2	=	Vickers microhardness coefficient
$D(r)$	=	macrogap profile, m
d	=	mean contacting bodies distance, m
E	=	Young's modulus, Pa
E'	=	effective elastic modulus, Pa
F	=	external force, N
H'	=	$c_1(1.62\sigma'/m)^{c_2}$, Pa
H^*	=	$c_1(\sigma'/m)^{c_2}$, Pa
Kn	=	Knudsen number
k	=	thermal conductivity, W/mK
l	=	depth, m
M	=	gas parameter, m
m	=	mean absolute surface slope
P	=	pressure, Pa
Pr	=	Prandtl number
Q	=	heat flow rate, W
q	=	heat flux, W/m^2
R	=	thermal resistance, K/W
r, z	=	cylindrical coordinates
T	=	temperature, K
Y	=	mean surface plane separation, m
α	=	nondimensional parameter $\equiv \sigma\rho/a_H^2$
α_T	=	thermal accommodation coefficient
γ	=	exponent of the general pressure distribution
γ_g	=	ratio of gas specific heats
δ	=	maximum surface out-of-flatness, m
Λ	=	mean free path, m
λ	=	nondimensional separation $\equiv Y/\sqrt{2}\sigma$
ν	=	Poisson's ratio
ξ	=	nondimensional radial position $\equiv r/a_L$
ρ	=	radius of curvature, m
σ	=	rms surface roughness, m
σ'	=	σ/σ_0, where $\sigma_0 = 1$ μm
τ	=	nondimensional parameter, identical to ρ/a_H
ω	=	bulk normal deformation, m

Subscripts

a	=	apparent
G	=	macrogap
g	=	gas, microgap
H	=	Hertz
j	=	joint
j, flat	=	flat joint
L	=	large, macrocontact
r	=	real
s	=	solid, micro
0	=	reference value
1, 2	=	solid 1, 2

Introduction

A SURFACE is characterized not only by the roughness but also by its curvature/out-of-flatness. When nonconforming random rough surfaces are placed in mechanical contact, due to the surface roughness, real contacts or microcontacts occur at the top of surface asperities. As a result of surface out-of-flatness or curvature, the microcontacts are distributed in the macrocontact area A_a. In addition, the contact pressure is not uniform and asymptotically approaches zero at the edge of the macrocontact area, $r = a_L$. In the real contact area A_r, the summation of microcontacts is typically a small fraction of the nominal contact area.

The geometry of nonconforming rough contacts is shown in Fig. 1, where two cylindrical solids with a radius of b_L are pressed against each other with an external load F. The gap between the contacting bodies is filled with an interstitial gas at pressure P_g and heat is being transferred from one body to another. Generally, heat transfer through the contact interface is not limited to conduction through the actual contact area. Rather, heat transfer across a solid joint can occur via three distinct modes, radiative transfer, conduction through interstitial material in the gap, and conduction through the real contact area. As mentioned in the first part of this study,[1] thermal radiation across the gap in most applications can be neglected; thus, the remaining heat transfer modes are conduction through the microcontacts and conduction through the interstitial

Received 26 September 2003; revision received 23 December 2003; accepted for publication 25 December 2003; presented as Paper 2004-0822 at the AIAA 42nd Aerospace Meeting and Exhibit, Reno, NV, 5–8 January 2004.

*Ph.D. Candidate, Department of Mechanical Engineering, Microelectronics Heat Transfer Laboratory.

†Distinguished Professor Emeritus, Department of Mechanical Engineering, Microelectronics Heat Transfer Laboratory. Fellow AIAA.

‡Associate Professor, Director, Microelectronics Heat Transfer Laboratory.

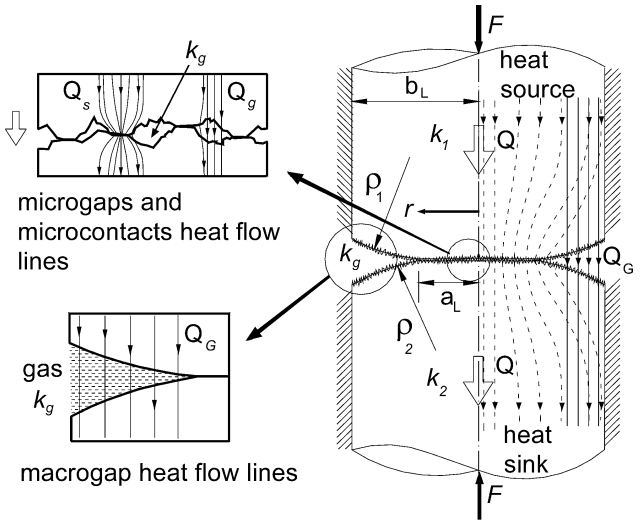

Fig. 1 Contact of nonconforming rough surfaces with presence of interstitial gas.

gas filling the gap between contacting bodies. As shown in Fig. 1, heat transfer occurs through three main paths, the interstitial gas within the microgap Q_g, microcontacts Q_s, and the interstitial gas within the macrogap, Q_G. As a result of the small real contact area and low thermal conductivities of interstitial gases, heat flow experiences a relatively large thermal resistance passing through the joint. This phenomenon leads to a relatively high-temperature drop across the interface.

The rate of heat transfer across the nonconforming rough joints depends on a number of parameters: thermal properties of solids and gas, elastic and plastic mechanical properties of solids, gas pressure, surface curvature or out-of-flatness, surface roughness characteristics, and applied load.

In applications where the contact pressure is relatively low, the real contact area is limited to an even smaller portion of the apparent area, that is, $A_r \sim 0.01 A_a$. Consequently, the heat transfer takes place mainly through the interstitial gas in the gap. The relative magnitude of the gap heat transfer varies greatly with the size of the macrocontact, applied load, surface roughness, gas pressure, and thermal conductivities of the gas and solids. As the contact pressure increases, the heat transfer through the microcontacts increases and becomes more significant. Many engineering applications of thermal contact resistance (TCR) are associated with low contact pressure with the presence of air (interstitial gas); therefore, modeling the nonconforming rough contacts with the presence of interstitial gas is an important issue.

To the authors' knowledge there are no compact analytical models for predicting TCR of the nonconforming rough joints in the presence of an interstitial gas in the literature. The objective of this work is to develop a comprehensive yet simple model for determining the heat transfer through the gap between nonconforming rough surfaces in the presence of an interstitial gas. A new approximate model is developed, which accounts for thermophysical properties of the interstitial gas and solids, gas pressure, mechanical properties of solids, applied load, surface roughness, and surface curvature/out-of-flatness. The model covers the entire range of gas conduction heat transfer modes, that is, continuum, slip, transition, and free molecular.

Solid–Solid TCR

Bahrami et al.[2] studied mechanical contact of nonconforming rough surfaces. A closed set of governing relationships was reported for spherical rough contacts and solved numerically. The surface curvature was approximated by a truncated spherical profile.[3] Then the actual contact geometry of the spheres was replaced by a flat surface and a profile, which resulted in the same undeformed gap between the surfaces.[4] Similar to Greenwood and Tripp,[5] the spherical profile was approximated by a parabolid in the contact region. The bulk deformation was assumed to be within the elastic limit of the solids, and the microcontacts were assumed to deform plastically. For convenience, all elastic deformations were considered to occur in one body, which had an effective elastic modulus, and the other body was assumed to be rigid. The effective elastic modulus and the equivalent radius of curvature can be found from

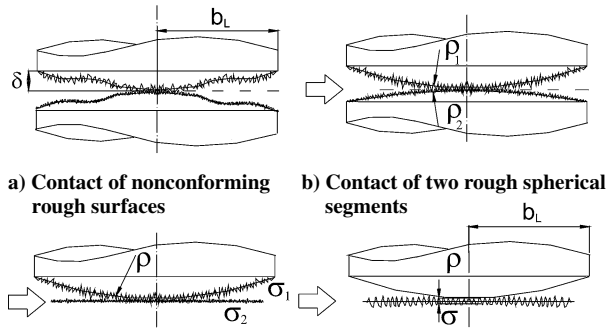

Fig. 2 Summary of geometrical modeling.

$$1/\rho = 1/\rho_1 + 1/\rho_2$$

$$1/E' = \left(1-\upsilon_1^2\right)\Big/E_1 + \left(1-\upsilon_2^2\right)\Big/E_2 \tag{1}$$

where subscripts 1 and 2 represent bodies 1 and 2. As discussed in Ref. 1, the contact between two Gaussian rough surfaces is modeled as the contact between a single Gaussian surface, having an effective surface characteristic, with a perfectly smooth surface, where the mean separation between two contacting planes, Y, remains the same. The equivalent roughness σ and surface slope m can be found from $\sigma = \sqrt{(\sigma_1^2 + \sigma_2^2)}$ and $m = \sqrt{(m_1^2 + m_2^2)}$. Figure 2 summarizes the geometrical model. Clausing and Chao[3] used an approximate geometrical relationship to relate the surface radius of curvature ρ to the maximum surface out-of-flatness δ, that is, $\rho = b_L^2/2\delta$. Note that this relationship can be used for relatively large radii of curvature.

Bahrami et al.[2] proposed a general contact pressure distribution that covers the complete range of spherical rough contacts including the Hertzian smooth limit. Simple correlations were developed for the maximum contact pressure P_0 and radius of the macrocontact a_L. When the Buckingham Π theorem was applied, it was shown that there are two important governing nondimensional parameters α and τ that describe the contact problem. The nondimensional roughness parameter α, defined by Johnson,[4] is the ratio of roughness over the Hertzian maximum bulk deformation $\omega_{0,H}$

$$\alpha = \sigma/\omega_{0,H} \equiv \sigma\rho\Big/a_H^2 = \sigma(16\rho E'^2/9F^2)^{\frac{1}{3}} \tag{2}$$

where $a_H = (0.75F\rho/E')^{1/3}$ is the Hertzian radius of contact, that is, the limiting contact case where both surfaces are ideally smooth. The other nondimensional parameter was chosen as

$$\tau = \rho/a_H = (4E'\rho^2/3F)^{\frac{1}{3}} \tag{3}$$

The general pressure distribution[2] is

$$P(\xi) = P_0(1-\xi^2)^{\gamma} \tag{4}$$

$$P_0 = P_{0,H}/(1 + 1.37\alpha\tau^{-0.075}) \tag{5}$$

$$a_L = 1.80 a_H\left(\sqrt{\alpha + 0.31\tau^{0.056}}\Big/\tau^{0.028}\right) \tag{6}$$

where $P_{0,H} = 1.5F/\pi a_H^2$, $\xi = r/a_L$, and $\gamma = 1.5(P_0/P_{0,H})(a_L/a_H)^2 - 1$ are the maximum Hertzian contact pressure, dimensionless radial position, and general pressure distribution exponent, respectively.

Bahrami et al.[6] using scale analysis methods developed an analytical model for determining the micro- and macrothermal resistances for contact of nonconforming rough surfaces in a vacuum. It was shown that the micro- and macrothermal resistances are in series, that is, $R_j = R_s + R_L$.

With the assumption of plastically deformed asperities, simple correlations were proposed[6] for predicting the microcontacts R_s and the macrocontact R_L thermal resistances in a vacuum,

$$R_s = \frac{0.565 H^*(\sigma/m)}{k_s F} \tag{7}$$

$$R_L = \frac{(1 - a_L/b_L)^{\frac{3}{2}}}{2 k_s a_L} \tag{8}$$

where

$$k_s = 2k_1k_2/(k_1 + k_2), \qquad H^* = c_1(\sigma'/m)^{c_2}$$

where $\sigma' = \sigma/\sigma_0$, where $\sigma_0 = 1\ \mu$m, c_1, c_2, k_s, and F are a reference value, correlation coefficients determined from the Vickers microhardness measurements (see Ref. 7), the harmonic mean of solid thermal conductivities, and the applied load, respectively.

Thermal Resistance of Interstitial Gas

The first part[1] of this work is dedicated to the development of an approximate simple model for predicting the conduction heat transfer through the microgap between conforming rough surfaces. Conduction heat transfer in a gas layer between two parallel plates is commonly categorized into four heat-flow regimes[8]: continuum, temperature jump or slip, transition, and free-molecular. The parameter that characterizes the regimes is the Knudsen number $Kn = \Lambda/d$, where Λ and d are the molecular mean free path and the distance separating the two plates, respectively. The molecular mean free path is defined as the average distance a gas molecule travels before it collides with another gas molecule, and it is proportional to the gas temperature and inversely proportional to the gas pressure,[9]

$$\Lambda = (P_0/P_g)(T_g/T_0)\Lambda_0 \tag{9}$$

where Λ_0 is the mean free path value at some reference gas temperature T_0 and pressure P_0.

Yovanovich[10] proposed that the heat transfer in a gas layer between two isothermal plates for all four flow regimes can be effectively calculated from

$$q_g = [k_g/(d + M)](T_1 - T_2) \tag{10}$$

where T_1, T_2, d, k_g, and q_g are the uniform temperatures and the distance between the two isothermal parallel plates, gas thermal conductivity, and the gap heat flux, respectively. The gas parameter M is defined as

$$M = [(2 - \alpha_{T1})/\alpha_{T1} + (2 - \alpha_{T2})/\alpha_{T2}][2\gamma_g/(1 + \gamma_g)](1/Pr)\Lambda \tag{11}$$

where α_{T1}, α_{T2}, γ_g, Pr, and Λ are thermal accommodation coefficients corresponding to the gas–solid combination of plates 1 and 2, ratio of the gas specific heats, gas Prandtl number, and molecular mean free path at P_g and T_g, respectively.

In the first part,[1] it was shown that the thermal joint resistance of conforming rough contacts can be considered as the parallel combination of the microcontacts and the interstitial gas thermal resistances, that is, $R_{j,\text{flat}} = (1/R_s + 1/R_g)^{-1}$. As already mentioned, due to the surface roughness the real contact area is a small portion of the apparent contact area, that is, $A_r \ll A_a$. When it was assumed that the microgap heat transfer area is equal to the apparent contact area, that is, $A_g = A_a$, it was shown that for conforming rough contacts $d = Y$, where Y is the separation between the mean planes of contacting surfaces. This simplified the microgap geometry. Therefore, the heat transfer through the interstitial gaps becomes equal to the heat transfer between two isothermal parallel plates located at the distance Y from each other, that is,

$$Q_g = [k_g \Delta T/(M + Y)]A_a \tag{12}$$

It was shown that[1]

$$\lambda = Y\Big/\sqrt{2}\sigma = \text{erfc}^{-1}(2P/H') \tag{13}$$

where $\text{erfc}^{-1}(\cdot)$, $H' = c_1(1.62\sigma'/m)^{c_2}$, $P = F/A_a$, and A_a are the inverse complementary error function, the effective microhardness, contact nominal pressure, and the apparent macrocontact area, respectively.

The inverse complementary error function $\text{erfc}^{-1}(x)$ can be determined from[1]

$$\text{erfc}^{-1}(x) = \begin{cases} \dfrac{1}{0.218 + 0.735x^{0.173}} & 10^{-9} \le x \le 0.02 \\ \dfrac{1.05(0.175)^x}{x^{0.12}} & 0.02 < x \le 0.5 \\ \dfrac{1 - x}{0.707 + 0.862x - 0.431x^2} & 0.5 < x \le 1.9 \end{cases} \tag{14}$$

The maximum relative difference between Eq. (14) and $\text{erfc}^{-1}(x)$ is less than 2.8% for the range $10^{-9} \le x \le 1.9$.

The approximate model developed in Ref. 1 was compared with more than 510 experimental data points collected by Hegazy[7] and Song.[11] Tests were performed with stainless steel (SS) 304 and nickel 200 with three gases: argon, helium, and nitrogen. The data covered a wide range of surface characteristics, applied load, thermal and mechanical properties, and gas pressure, which was varied from vacuum to atmospheric pressure. The model showed good agreement with the data over entire range of comparison. The rms difference between the model and data was determined to be approximately 7.3%.

Present Model

The modeled geometry of the contact is shown in Fig. 3. The actual contact of two nonconforming rough surfaces is simplified to the contact of a flat rough, having the equivalent surface roughness σ, surface slope m, microhardness H', and the effective elastic modulus E', with a smooth rigid spherical profile that has the equivalent radius of curvature ρ. It is assumed that the contacting surfaces have Gaussian roughness and the asperities deform plastically; the bulk material deforms elastically. It is assumed that the contact planes are isothermal.

Total heat flow through the joint includes the heat transfer through 1) solids or microcontacts, Q_s, 2) the microgap within the macrocontact area, Q_g, and 3) the macrogap between noncontacting parts of bodies, Q_G.

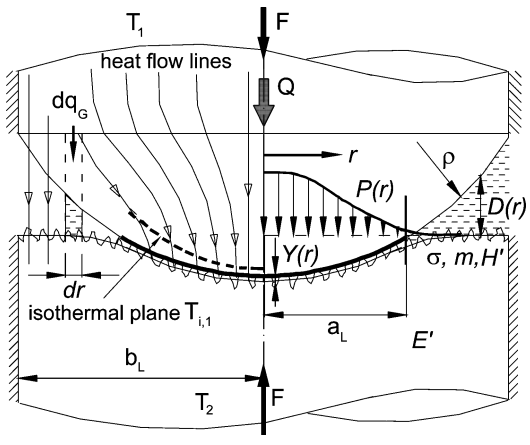

Fig. 3 Nonconforming rough joint heat transfer in gaseous environment.

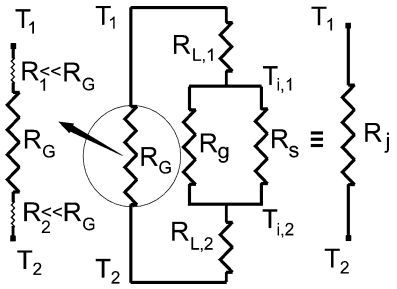

Fig. 4 Thermal resistance network, nonconforming rough joint.

TCR of nonconforming rough surfaces with the presence of interstitial gas contains four thermal resistance components: 1) the macrocontact constriction/spreading resistance R_L, 2) the microcontacts constriction/spreading resistance R_s, 3) resistance of interstitial gas in the microgap, R_g, and 4) thermal resistance of interstitial gas in the macrogap, R_G.

The effective microcontacts and the macrocontact thermal resistances, that is, R_s and R_L, can be determined using Eqs. (7) and (8), respectively.

Microcontacts can be modeled as isothermal heat sources on a half-space. When circular microcontacts with the radius a_s on the order of micrometers are considered, isothermal planes with some intermediate temperatures $T_{i,1}$ and $T_{i,2}$ at depth l must exist in bodies 1 and 2, respectively (Fig. 3). For example in body 1, it can be written that $T_1 < T_{i,1} < T_{c,1}$, where $T_{c,1}$ is the contact plane temperature. Under vacuum condition, the distance between the isothermal planes and the contact plane is $l = 40a_s \sim 40\ \mu$m (Ref. 12). Macrocontact thermal constriction/spreading resistances $R_{L,1}$ and $R_{L,2}$ can be considered in series between the heat source T_1 and the isothermal plane $T_{i,1}$ and the isothermal plane $T_{i,2}$ and the heat sink T_2, respectively. By the increase of the gas pressure, heat flow through the microgap increases and the distance l decreases. The macrogap, the gap between the noncontacting area of the sphere and the flat, provides a parallel path for transferring heat from the heat source to the sink. Figure 4 shows the thermal resistance network for a nonconforming rough contact. Therefore, the thermal joint resistance can be written as

$$R_j = \left\{1\Big/\left[(1/R_s + 1/Rg)^{-1} + R_L\right] + 1/R_G\right\}^{-1} \qquad (15)$$

where $R_L = R_{L,1} + R_{L,2}$ is the macrocontact constriction/spreading thermal resistance.

The macrogap thermal resistance is considered to provide a parallel path between the heat source and the sink. As shown in Fig. 4, R_G has three components: the macrogap resistance and R_1 and R_2 corresponding to the bulk thermal resistance of the solid layers in bodies 1 and 2, respectively. The bulk resistances R_1 and R_2 can be considered negligible in relation to R_G because the gas thermal conductivity is much lower than in the solids, that is, $k_g/k_g \leq 0.01$.

Microgap Thermal Resistance R_g

To determine the gas heat transfer through the microgap, the macrocontact area is divided into infinitesimal surface elements dr where the contact pressure can be assumed uniform. Therefore, the conforming rough microgap relationship Eq. (12) can be used for each surface element. By integrating the local heat flow through the interstitial gas in the microgap over the macrocontact area, we obtain

$$Q_g = \int\int \frac{k_g(T_{i,1} - T_{i,2})}{Y(r) + M}\, \mathrm{d}A_g \qquad (16)$$

Note that the microgap resistance R_g accounts for the resistance between two isothermal planes at temperatures, $T_{i,1}$ and $T_{i,2}$ (Fig. 3). (For more details, see Ref. 1.) The macrocontact area is a circle with radius a_L because $A_g = A_a - A_r$ and $A_r \ll A_a$. Thus one can write $\mathrm{d}A_g = \mathrm{d}A_a = 2\pi r\, \mathrm{d}r$. When the definition of thermal resistance, that is, $R_g = (T_{i,1} - T_{i,2})/Q_g$ and Eq. (16) are used, the microgap thermal resistance can be written as

$$R_g = \frac{1}{2\pi k_g}\left[\int_0^{a_L} \frac{r\, \mathrm{d}r}{Y(r) + M}\right]^{-1} \qquad (17)$$

To determine R_g, the local plane separation $Y(r)$ is required. The governing relationships and the numerical algorithm to calculate $Y(r)$ were explained by Bahrami et al.[2] To avoid a numerical solution, an approximate expression for the nondimensional separation is developed by using the general pressure distribution correlation.

Because of surface curvature, the plane separation Y is not uniform throughout the macrocontact. It has its minimum at the center of the contact and increases as radial position r increases. When an infinitesimal surface element dr is considered, where contact pressure can be considered uniform, the local nondimensional plane separation using Eq. (13) is

$$2P(\xi)/H' = \mathrm{erfc}\,\lambda(\xi) \qquad (18)$$

where $\lambda(\xi) = Y(\xi)/\sqrt{2}\sigma$ and $\xi = r/a_L$ are the nondimensional plane separation and the nondimensional radial position, respectively.

The general pressure distribution satisfies the following conditions: 1) $\mathrm{d}P(\xi)/\mathrm{d}\xi = 0$, at $\xi = 0$, contact is axisymmetric; 2) $P(\xi) = P_0$, at $\xi = 0$, the maximum contact pressure is known, that is, Eq. (5); and 3) $P(\xi)/P_0 \approx$ negligible, at $\xi = 1$, the contact pressure is negligible at $r = a_L$.

When a parabolic shape is assumed for $\lambda(\xi)$ and the preceding conditions and Eq. (18) are used, an expression for $\lambda(\xi)$ can be found as

$$\lambda(\xi) = a_1 + a_2\xi^2 \qquad (19)$$

where

$$a_1 = \mathrm{erfc}^{-1}(2P_0/H'), \qquad a_2 = \mathrm{erfc}^{-1}(0.03P_0/H') - a_1$$

where P_0 is given by Eq. (5). Equation (19) is compared with the numerical output of the computer program discussed in Ref. 2 in Fig. 5, for a typical contact. As shown, the agreement between Eq. (19) and the numerical results[2] is reasonable.

Substitute Eq. (19) into Eq. (17). After the integral is evaluated and simplified, R_g can be found from

$$R_g = \frac{\sqrt{2}\sigma a_2}{\pi k_g a_L^2\, \ell_n\left[1 + a_2\Big/\left(a_1 + M\Big/\sqrt{2}\sigma\right)\right]} \qquad (20)$$

In the conforming rough limit where surfaces are flat $\rho \to \infty$, $a_L \to b_L$, the pressure distribution becomes uniform over the macrocontact area, that is, $\mathrm{d}P/\mathrm{d}r = 0$, and $P = P_0 = F/\pi b_L^2$. Consequently, the mean separation Y will be uniform throughout the

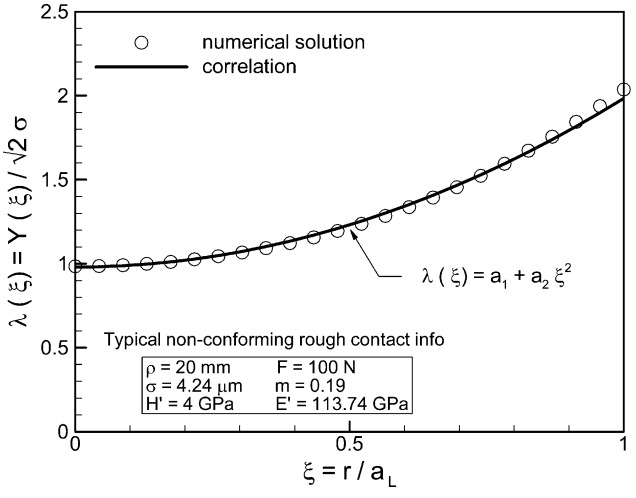

Fig. 5 Nondimensional separation, nonconforming rough joint.

macrocontact area. When the preceding conditions for the general pressure distribution are used, $a_2 = 0$ and $a_1 = \text{erfc}^{-1}(2P/H')$. Substituting these new values into Eq. (20) and using L'Hopital's rule, one finds

$$\lim_{a_2 \to 0} R_g = \frac{Y + M}{k_g A_a}$$

which is the conforming microgap thermal resistance developed in the first part of this study.[1] Note that, for conforming rough contacts, $\text{erfc}^{-1}(2P/H') = \lambda = Y/\sqrt{2}\sigma$.

Macrogap Thermal Resistance R_G

The macrogap area A_G is divided into infinitesimal surface elements dr. The heat transfer through the interstitial gas in the macrogap, Q_G, can be determined using Eq. (12),

$$Q_G = \int\int \frac{k_g(T_1 - T_2)}{D(r) + M}\, \mathrm{d}A_G \tag{21}$$

where $D(r)$, T_1, and T_2 are the sphere profile in the noncontacting region and the heat source and sink temperatures, respectively. Using the definition of thermal resistance, that is, $R_G = (T_1 - T_2)/Q_G$, one obtains

$$R_G = \frac{1}{2\pi k_g}\left[\int_{a_L}^{b_L} \frac{r\, \mathrm{d}r}{D(r) + M}\right]^{-1} \tag{22}$$

The macrogap profile of a sphere–flat contact with the radius ρ and the maximum deformation ω_0 is shown in Fig. 6. Even though the normal stress (contact pressure) is zero (negligible) beyond the macrocontact area, due to shear stress in the elastic half-space the normal deformation at the edge of the macrocontact is not zero. However, in this study for convenience, that deformation is neglected, that is, $\omega(r = a_L) = 0$. The maximum normal deformation ω_0 is much smaller than the radius of the sphere, $\omega_0 \ll \rho$. Thus in the right triangle OCB (Fig. 6), one can write

$$\omega_0 = a_L^2 \big/ 2\rho \tag{23}$$

The profile of the circle $D(r)$ with the radius ρ and the center coordinate $(0, \rho - \omega_0)$ is

$$D(r) = \rho - \omega_0 - \sqrt{\rho^2 - r^2} \tag{24}$$

where $a_L \le r \le b_L$.

Substitute Eq. (24) into Eq. (22). After the integral is evaluated and simplified,

$$2\pi k_g R_G = 1/\{S\, \ell n[(S - B)/(S - A)] + B - A\} \tag{25}$$

where $A = \sqrt{(\rho^2 - a_L^2)}$, $B = \sqrt{(\rho^2 - b_L^2)}$, and $S = \rho - \omega_0 + M$.

It can be seen that in the conforming limit where $\rho \to \infty$, consequently $a_L \to b_L$, the macrogap resistance $R_G \to \infty$.

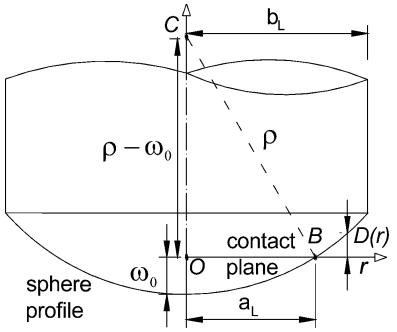

Fig. 6 Macrogap geometry.

Parametric Study

The influence of the main input parameters on the thermal joint resistance of a typical contact, indicated in Table 1, is investigated. The effects of external load F, surface roughness σ, gas pressure P_g, and surface radius of curvature ρ on the joint thermal resistance and its components are plotted in Figs. 7–10, respectively. The contacting surfaces are SS, and the interstitial gas is nitrogen at 300 K and 200 torr. The trends of the model are studied for a range of each input parameter, while the remaining parameters in Table 1 are held constant.

As shown in Fig. 7, with relatively small loads, due to the small size and number of microcontacts, the microcontact resistance R_s

Table 1 Input parameters for a typical SS–nitrogen contact

Parameter	Value
$\alpha_T\ (SS - N_2)$	0.78
b_L	12 mm
ρ	20 mm
P_g	200 torr
σ	4.24 μm
m	0.19
F	100 N
Λ_0	62.5 nm
k_g	0.026 W/mK
T_g	300 K
k_s	20 W/mK
c_1, c_2	4 GPa, 0

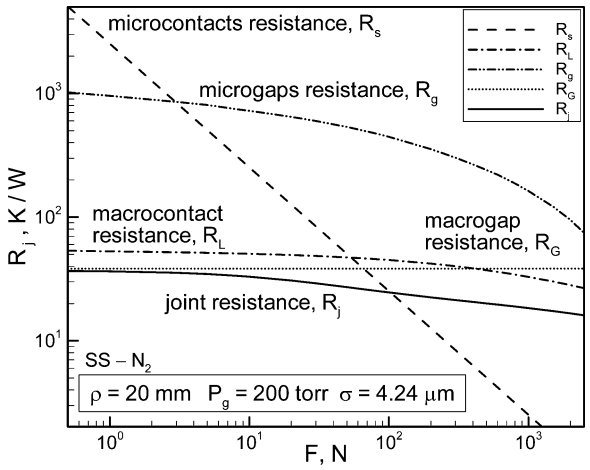

Fig. 7 Effect of load on thermal joint resistance.

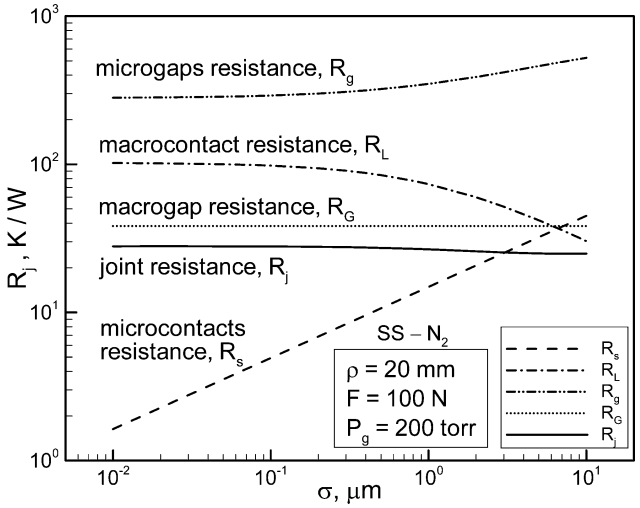

Fig. 8 Effect of roughness on thermal joint resistance.

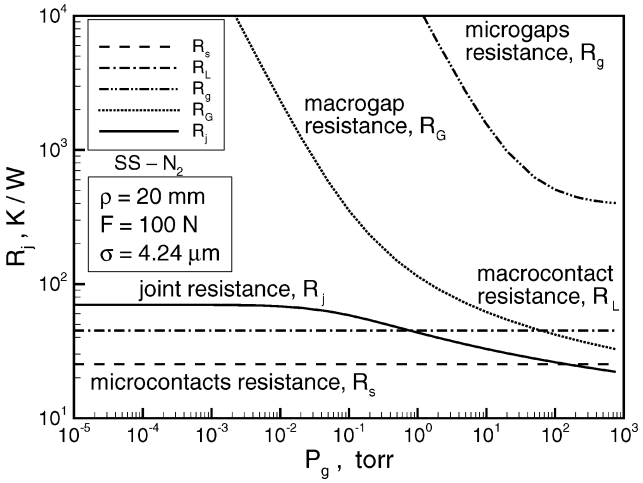

Fig. 9 Effect of nitrogen pressure on thermal joint resistance.

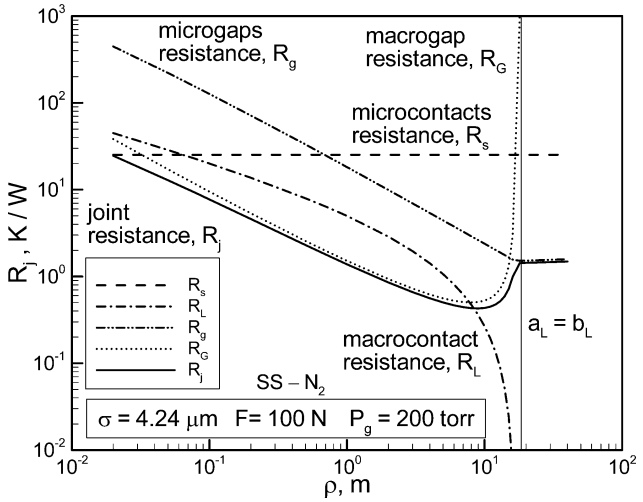

Fig. 10 Effect of radius of curvature on thermal joint resistance.

is large, also the separation between the two bodies is large; thus, the microgap resistance R_g is high. At relatively light loads, the macrocontact area is small; thus, the macrocontact resistance R_L is large. It can be seen that, at relatively light loads, the joint resistance is close to the macrogap resistance. In other words, most of the heat transfer takes place through the interstitial gas in the macrogap. When the applied load is increased, 1) the microcontacts resistance R_s decreases linearly [Eq. (7)], 2) the separation between the mean planes decreases, which results in a decrease in the microgap resistance R_g; 3) the radius of the macrocontact a_L is increased, which leads to a decrease in the macrocontact resistance R_L [Eq. (8)]; and 4) the macrogap thermal resistance R_G increases (slightly). The joint resistance [Eq. (15)] decreases as the external load increases.

The effect of surface roughness σ is shown in Fig. 8. As surface roughness is increased, while other contact parameters are held constant, 1) the separation between the two mean planes Y increases, thus, the microgap resistance R_g increases; 2) the microcontacts resistance R_s increases linearly [Eq. (7)]; and 3) there is an increase in the macrocontact area, which leads to a lower macrocontact resistance R_L and higher (slightly in this case) macrogap resistance R_G. In total, increasing surface roughness results in a decreases in the joint resistance (for this contact).

The gas pressure is varied from vacuum to the atmospheric pressure, and the joint resistance and its components are plotted in Fig. 9. The microcontacts R_s and the macrocontact R_L thermal resistances remain unchanged as the gas pressure varies. The macrogap R_G and the microgap R_g thermal resistances approach infinity for vacuum conditions; thus, the joint resistance becomes simply the summation of the microcontacts R_s and macrocontact R_L resistances [Eq. (15)]. As the gas pressure increases, the gap resistances R_g and R_G drop; as a result, the joint resistance decreases.

Figure 10 shows the effect of surface curvature on the joint resistance. As the radius of curvature increases, the radius of the macrocontact area a_L increases. Consequently, the macrocontact resistance R_L decreases. An increase in the radius of the macrocontact area leads to a decrease in the microgap resistance R_g [Eq. (20)]. The dependency of the macrogap resistance R_G on the radius of curvature is complex. As the radius of curvature increases, the macrogap resistance decreases to a minimum. Any furthur increase in the radius results in an increase in the macrogap resistance. In the limit, where the contacting surfaces become flat, that is, $a_L \to b_L$, the macrogap resistance approaches infinity, and the macrocontact resistance goes to zero. The joint resistance then becomes the parallel combination of the microcontacts and the microgaps thermal resistances, that is, the conforming rough joint resistance. Additionally, it can be seen that for a prescribed load and gas pressure a surface curvature exists that minimizes the joint resistance. It can also be seen that the microcontact resistance R_s is not a function of surface curvature. See Bahrami et al.[6] for more detail.

Comparison with Experimental Data

The present model is compared with more than 110 experimental data points collected by Kitscha.[13] The geometry of the experimental setup is shown in Fig. 3. Two spherical carbon steel samples (radii 12.7 and 25.4 mm) and a steel-1020 flat specimen with surface roughness of $\sigma = 0.127$ μm were used. Specimens were cylindrical with the same radius, $b_L = 12.7$ mm. Samples were placed in contact by applying external loads in a chamber filled with an interstitial gas. To minimize the radiation and convection heat transfer to the surroundings, lateral surfaces of specimens were insulated. The interstitial gases were air and argon. The gas pressure was varied from vacuum $\approx 10^{-5}$ to 700 torr. Table 2 summarizes the experiment numbers, specimen radius of curvature, gas, and range of applied load of the Kitscha experimental data.[13]

The mean contact temperature, that is, the mean gas temperature, was maintained at approximately 40°C; the harmonic mean thermal conductivities of the specimens was reported as 49 W/mK. Thermal properties of argon and air are listed in Table 3.[11] Note that the reference mean free paths Λ_0 are at 288 K and 760 torr and temperature in k_g correlations must be in Kelvin.

Tests were conducted at different external loads, at each load the gas pressure increased from vacuum (approximately 10^{-5}) to 700 torr while the load was held constant. Figure 11 shows the comparison between the present model and Kitscha's[13] experimental data. For each data set, the radius of curvature, load, and interstitial gas are indicated, for example, ρ12-F56Air means, radius of curvature was $\rho = 12.7$ mm, applied load was $F = 56$ N, and the interstitial gas was air. The horizontal axis is the thermal joint resistance predicted by the model, that is, Eq. (15), and the vertical axis shows the experimental data. Therefore, the model is shown by the 45-deg line; also ±15% bounds of the model are included in the comparison. As shown in Fig. 11, the data show good agreement with the model. The relative rms difference between the model and the data is approximately 7.2%.

Table 2 Summary of Kitscha experiments[13]

Test	ρ, mm	Gas	F, N
T1	12.7	Air	16.7–467
T2	25.4	Air	16.9–135
T3	12.7	Argon	17.8–467

Table 3 Properties of air and argon

Gas	k_g, W/mK	Pr	α_T	γ_g	Λ_0, nm
Air	$0.0021 + 8 \times 10^{-5} T$	0.70	0.87	1.39	64.01
Ar	$0.0159 + 4 \times 10^{-6} T$	0.67	0.9	1.67	66.55

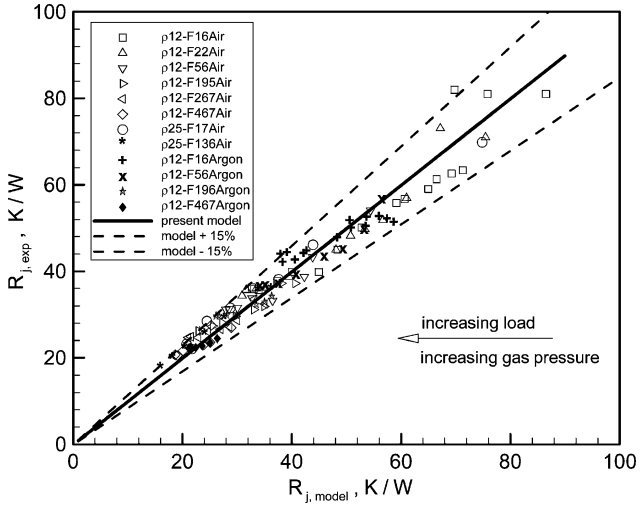

Fig. 11 Comparison of present model with Kitscha data.[13]

Conclusions

An approximate analytical model was developed for determining TCR of nonconforming random rough contacts in the presence of an interstitial gas. Uniform temperatures for the contacting surfaces were assumed. With use of the general pressure distribution,[2] a relationship for local separation was developed. When this relationship in the conforming rough gap model developed in the first part of this study[1] was employed, a relationship for microgap thermal resistance of nonconforming rough contacts was derived.

An expression for the macrogap resistance was found by integrating local heat transfer over the noncontacting parts of contacting bodies. The present model covers the four regimes of heat conduction modes of gas, that is, continuum, temperature-jump or slip, transition, and free molecular and accounts for gas and solid mechanical and thermal properties, gas pressure and temperature, surface roughness, surface curvature, and applied load.

The effects of the main input parameters on the joint thermal resistances and its components predicted by the model were plotted and discussed. In particular, it was shown that for a rough sphere–flat contact at relatively light loads most of the heat transfer take place through the interstitial gas in the macrogap. This demonstrates the importance of the macrogap heat transfer, especially in light loads. The surface curvature has two competing effects on the joint resistance. It was observed that, by increasing surface curvature, the macrocontact and the macrogap and consequently the joint resistance decrease up to a certain value of surface curvature. As the surfaces approach the flat surface, the macrocontact resistance approaches zero, whereas the macrogap resistance approaches infinity. As a result of this trend, it was seen that a surface curvature exists that minimizes the joint resistance, while other contact parameters are held constant.

The present model was compared with 110 experimental data points collected by Kitscha.[13] Tests were performed with carbon steel and steel-1020 with air and argon. The gas pressure was varied from vacuum to (almost) atmospheric pressure. The present model showed good agreement with the data over the entire range of the comparison. The rms relative difference between the model and data was determined to be approximately 7.3%.

References

[1]Bahrami, M., Yovanovich, M. M., and Culham, J. R., "Thermal Joint Resistance of Conforming Rough Surfaces with Gas-Filled Contacts," *Journal of Thermophysics and Heat Transfer*, Vol. 18, No. 3, 2004, pp. 325–332; also AIAA Paper 2004-0821, Jan. 2004.

[2]Bahrami, M., Culham, J. R., Yovanovich, M. M., and Schneider, G. E., "Thermal Contact Resistance of Non-Conforming Rough Surfaces Part 1: Mechanical Model," AIAA Paper 2003-4197, June 2003.

[3]Clausing, A. M., and Chao, B. T., "Thermal Contact Resistance in a Vacuum Environment," *Journal of Heat Transfer*, Vol. 87, 1965, pp. 243–251; also American Society of Mechanical Engineers, ASME Paper 64-HT-16, May 1964.

[4]Johnson, K. L., *Contact Mechanics*, Cambridge Univ. Press, Cambridge, England, U.K., 1985, Chap. 4.

[5]Greenwood, J. A., and Tripp, J.H., "The Elastic Contact of Rough Spheres," *Journal of Applied Mechanics*, Vol. 89, No. 1, 1967, pp. 153–159.

[6]Bahrami, M., Culham, J. R., and Yovanovich, M. M., "A Scale Analysis Approach to Thermal Contact Resistance," American Society of Mechanical Engineers, ASME Paper IMECE2003-44097, July 2003.

[7]Hegazy, A. A., "Thermal Joint Conductance of Conforming Rough Surfaces: Effect of Surface Micro-Hardness Variation," Ph.D. Dissertation, Dept. of Mechanical Engineers, Univ. of Waterloo, Waterloo, ON, Canada, 1985.

[8]Springer, G. S., "Heat Transfer in Rarefied Gases," *Advances in Heat Transfer*, Vol. 7, 1971, pp. 163–218.

[9]Kennard, E. H., *Kinetic Theory of Gases*, McGraw–Hill, New York, 1938, Chap. 8.

[10]Yovanovich, M. M., "Thermal Contact Correlations," *Spacecraft Radiative Transfer and Temperature Control*, edited by T. E. Horton, Progress in Aeronautics and Aerodynamics, Vol. 83, AIAA, New York, 1982, pp. 83–95; also AIAA Paper 81-1164, 1981.

[11]Song, S., "Analytical and Experimental Study of Heat Transfer Through Gas Layers of Contact Interfaces," Ph.D. Dissertation, Dept. of Mechanical Engineers, Univ. of Waterloo, Waterloo, ON, Canada, 1988.

[12]Bejan, A., and Kraus, D., *Heat Transfer Handbook*, Wiley, New York, 2003, Chap. 4.

[13]Kitscha, W., *Thermal Resistance of the Sphere-Flat Contact*, M.S. Thesis, Dept. of Mechanical Engineering, Univ. of Waterloo, Waterloo, Canada, ON, 1982.